EUROPEAN ORGANIZATION FOR NUCLEAR RESEARCH

CERN - PS DIVISION

THE MAGNETIC QUADRUPOLE PICK-UPS IN THE CERN PS

Andreas Jansson

Abstract

The idea of using non-linearities of beam position monitors to measure the second moment $\sigma_x^2 - \sigma_y^2$ of the transverse beam distribution is almost as old as the synchrotron. However, although a few successful experiments have been reported, the method has not become widely accepted. One reason for this has been that little or no effort was put into optimising the pick-ups that were used for the new purpose. In a standard beam position pick-up, the signal from the second moment is extremely weak and embedded in a strong common-mode background. Separating the signal from the background has therefore been a major stumbling block. Driven by the need for a non-destructive measurement of injection matching to preserve the small emittance of the LHC beam, a dedicated quadrupole pick-up has been developed for the CERN PS. The design employs magnetic coupling in a special pick-up geometry to remove the otherwise dominating background signal, thereby reducing the common-mode rejection requirements by about 60dB. Two pick-ups have been installed in the machine. When the data from these pick-ups is combined, it is possible to measure both the matching parameters and the emittance of each bunch in the injected beam. This paper gives an overview of the pick-up design, describes the methods used to analyse the data, and presents some measurement results, including comparisons with other instruments in the machine.

The Magnetic Quadrupole Pick-Ups in the CERN PS

Andreas Jansson

European Organization for Nuclear Research (CERN),
CH-1211 Geneva 23, Switzerland

Abstract. The idea of using the non-linearities of beam position monitors to measure the second moment $\sigma_x^2 - \sigma_y^2$ of the transverse beam distribution is almost as old as the synchrotron. However, although a few successful experiments have been reported, the method has not become widely accepted. One reason for this has been that little or no effort was put into optimizing the pick-ups that were used for the new purpose. In a standard beam position pick-up, the signal from the second moment is extremely weak and embedded in a strong common-mode background. Separating the signal from the background has therefore been a major stumbling block. Driven by the need for a non-destructive measurement of injection matching to preserve the small emittance of the LHC beam, a dedicated quadrupole pick-up has been developed for the CERN PS. The design employs magnetic coupling in a special pick-up geometry to remove the otherwise dominating background signal, thereby reducing the common-mode rejection requirements by about 60 dB. Two pick-ups have been installed in the machine. When the data from these pick-ups is combined, it is possible to measure both the matching parameters and the emittance of each bunch in the injected beam. This paper gives an overview of the pick-up design, describes the methods used to analyze the data, and presents some measurement results, including comparisons with other instruments in the machine.

INTRODUCTION

In any accelerator or storage ring, position pick-ups are standard diagnostic devices. A typical pick-up of the electrostatic type is shown in Figure 1 and consists of four electrodes around the beam. The passing beam induces a signal on each of these electrodes,
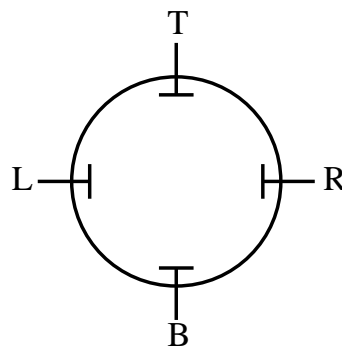

FIGURE 1. A typical position pick-up (electrostatic). The beam passes perpendicular to the plane of the drawing.

and the individual electrode signals can be combined in four (linearly independent) ways

$$\Sigma \quad = T + R + B + L \tag{1}$$

$$\Delta_{\mathrm{H}} = \quad R \quad -L \tag{2}$$

$$\Delta_{\mathrm{V}} = T \quad -B \tag{3}$$

$$\Xi \quad = T - R + B - L \tag{4}$$

where to lowest order

$$\Sigma = Z_\Sigma I, \quad \Delta_{\mathrm{H}} = Z_\Delta I \bar{x}, \quad \Delta_{\mathrm{V}} = Z_\Delta I \bar{y}, \quad \Xi = Z_\Xi I \kappa. \tag{5}$$

Here, I is the beam current and $(\bar{x}, \bar{y})$ the beam position relative to the pick-up centre in the horizontal and vertical plane, respectively. The Z coefficients are the so-called transfer impedances, and depend on the pick-up geometry. From this, the beam position can be determined as

$$\bar{x} = \frac{Z_\Sigma}{Z_\Delta} \frac{\Delta_{\mathrm{H}}}{\Sigma}, \quad \bar{y} = \frac{Z_\Sigma}{Z_\Delta} \frac{\Delta_{\mathrm{V}}}{\Sigma}. \tag{6}$$

The fourth possible signal combination Ξ, called the quadrupole signal, is not used in a position pick-up. However, it can be shown that

$$\kappa = \iint (x^2 - y^2) \rho(x, y) \, dx \, dy = \sigma_x^2 - \sigma_y^2 + \bar{x}^2 - \bar{y}^2. \tag{7}$$

The so-called quadrupole moment κ (in some references it is given the somewhat incorrect name 'second moment') is of interest since it provides information on the beam size. A pick-up that measures κ is often referred to as a quadrupole pick-up.

The idea of a quadrupole pick-up was first introduced by Gol'din[1] in a 1966 theoretical paper written in Russian. His ideas were taken up by Nassibian at CERN, who generalized the theory to higher-order field components[2] and pointed out the basic limitations of the method. A prototype was even built for the CERN Booster, but was never used.

The first experimental use of quadrupole pick-ups was reported in 1983, when Miller et al[3] used six strip-line BPMs distributed along the SLC linac to measure the emittance of the passing beam. To calculate the emittance from the pick-up readings, they solved a matrix equation derived from the linac optics. More recently, it was realized that this type of equations is often numerically unstable[4], and that a stable implementation of the method may require multiple measurements with different optics[5].

In rings, the use of quadrupole pick-ups has largely focused on the frequency content of the raw signal. Beam width oscillations produce sidebands to the revolution frequency harmonics in the quadrupole signal, at a distance of twice the betatron frequency, and this can be used to detect higher order instabilities as well as injection mismatch. This was done at the CERN Anti-proton Accumulator[6], where the phase and amplitude of the detected signals were also used to find a proper correction to the injection mismatch, using an empirical response matrix[7]. Similar measurements were later performed at the Fermilab Anti-proton Accumulator[8] and in the Low Energy Anti-proton Ring at

CERN[9]. However, measurements based on frequency analysis are complicated by the fact that the interesting sidebands can also be produced by position oscillations, which demands a very good injection steering.

Although quite a few papers have been published over the years, very little work has been done to adapt and optimize the design of the pick-up itself for measuring beam size. The typical approach has been to use existing beam position pick-ups, and to extract the quadrupole signal using sophisticated electronics. This lack of detector development may be one of the reasons why quadrupole pick-ups have remained 'exotic' instruments.

WHY MAGNETIC COUPLING?

There are two main problems associated with quadrupole pick-ups. The first is that the quadrupole moment κ is not only dependent on the beam dimensions, but also on the beam position. This is a fundamental problem which cannot be solved by optimizing the pick-up design. However, the problem can be circumvented by measuring the beam position and subtracting its contribution from the quadrupole moment. This is possible with reasonable accuracy as long as the beam displacement from the centre is small compared to the beam dimensions.

The second and more serious problem is the range in signal levels involved. In a typical position pick-up, the Σ signal is very much stronger than the Ξ signal, and this difference grows rapidly with the aperture to beam-size ratio. Since in reality only a finite accuracy can be obtained when combining the four electrode signals, this sets a limit to the measurement of the quadrupole moment.

At first glance, it may seem that this second problem is also fundamental. However, it can be circumvented by using a magnetic detector. The magnetic field created by an infinitely long beam of constant cross-section is, when written in cylindrical (ρ, θ) coordinates[10],

$$\vec{B}(\rho, \theta) = -I \frac{\mu_0}{2\pi} \left[\frac{1}{\rho} \hat{\theta} + \bar{x} \left(\frac{\cos\theta}{\rho^2} \hat{\theta} - \frac{\sin\theta}{\rho^2} \hat{\rho} \right) + \bar{y} \left(\frac{\sin\theta}{\rho^2} \hat{\theta} + \frac{\cos\theta}{\rho^2} \hat{\rho} \right) + \right.$$
$$\left. + (\sigma_x^2 - \sigma_y^2 + \bar{x}^2 - \bar{y}^2) \left(\frac{\cos 2\theta}{\rho^3} \hat{\theta} - \frac{\sin 2\theta}{\rho^3} \hat{\rho} \right) + \ldots \right] \quad (8)$$

The first term, corresponding to the monopole mode, is responsible for the Σ signal. This field mode has a field component only in the $\hat{\theta}$ direction. Thus, by designing a detector that measures only the radial component, the dominating signal can be entirely suppressed. Such a coupling is achieved by shaping the antenna loops as a cylinder around the beam. To maximize the sensitivity to the quadrupole field mode, the four antenna loops should then be positioned where its radial component is strongest, i.e. at $45°$ angle to the horizontal plane (see Figure 2).

If the loops measuring the radial field component have an azimuthal opening angle of ϕ, the transfer impedances can be expected to scale as[10]

$$Z_\Delta \propto \left(1 - \frac{a^2}{d^2} \right) \frac{\sin\frac{\phi}{2}}{a^2}, \qquad Z_\Xi \propto \left(1 - \frac{a^4}{d^4} \right) \frac{\sin\phi}{a^3}, \qquad (9)$$
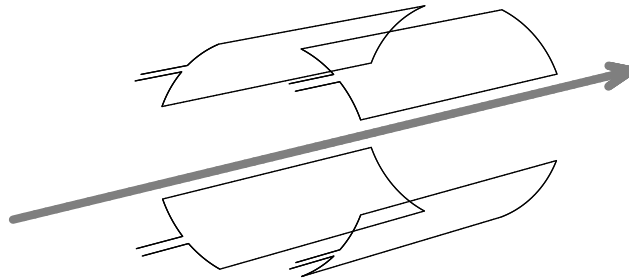
FIGURE 2. Arrangement of antenna loops to couple to the radial component of the magnetic field. The arrow symbolizes the beam.

where d is the radial position of the loops. Here, the effect of a conducting boundary at radial position a has also been taken into account.

PRACTICAL IMPLEMENTATION

To maximize the signal, the antenna loops should be placed as close as possible to the beam, and their preferred position is therefore given by the machine aperture.

When designing a magnetic quadrupole pick-up for the CERN PS, however, the antenna loops were placed a little further away, to make space for a ceramic vacuum tube inside the loops. The main reason was to avoid vacuum feed-throughs that could reduce the low-frequency response of the pick-up by introducing a parasitic series impedance in the antenna loops circuit. The ceramic was made circular for symmetry reasons, and was coated with a thin layer of titanium on the inside. The resistive layer acts as a shunt, significantly reducing the high frequency impedance of the pick-up, while being transparent in the passband of the pick-up.

A cylindrical cavity encloses the loops, providing continuity for the low frequency image currents. The space between ceramic and the cavity walls is divided longitudinally
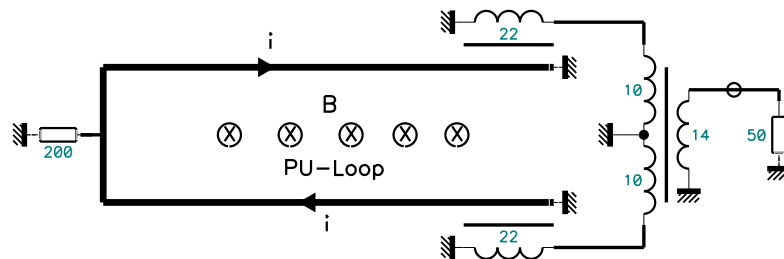

FIGURE 3. Schematic layout of one antenna loop, showing the transformer arrangement, the winding ratios and the position and value of the termination resistance.

in four sections by thin metal vanes. These shorten the path of the image currents, thereby further reducing the inductance seen by the beam. However, since they are placed in the symmetry planes of the quadrupole field, they do not affect the Ξ transfer impedance of the pick-up.

The four antenna loops were made of parallel, inter-connected rods, with an azimuthal opening angle ϕ of $45°$. The current induced in each loop is read out with a series of transformers (see Figure 3). These also act as impedance transformers, to improve the low frequency response by reducing the load seen by the loop. The transformer end of the loop is connected to ground, to reduce capacitive coupling between windings. At the other end of the loop, a second ground point is connected via a resistor, with the purpose of damping out loop resonances.

The four antenna loop signals from the pick-up are combined in a passive $50\,\Omega$ hybrid. Due to the pick-up geometry, the signal combination is different from the case of an electrostatic pick-up

$$\Delta_H = TR - BR - BL + TL \tag{10}$$

$$\Delta_V = TR + BR - BL - TL \tag{11}$$

$$\Xi = TR - BR + BL - TL \tag{12}$$

where TR is the top right loop, BL the bottom left etc. The Σ signal is zero by design, and is not used.
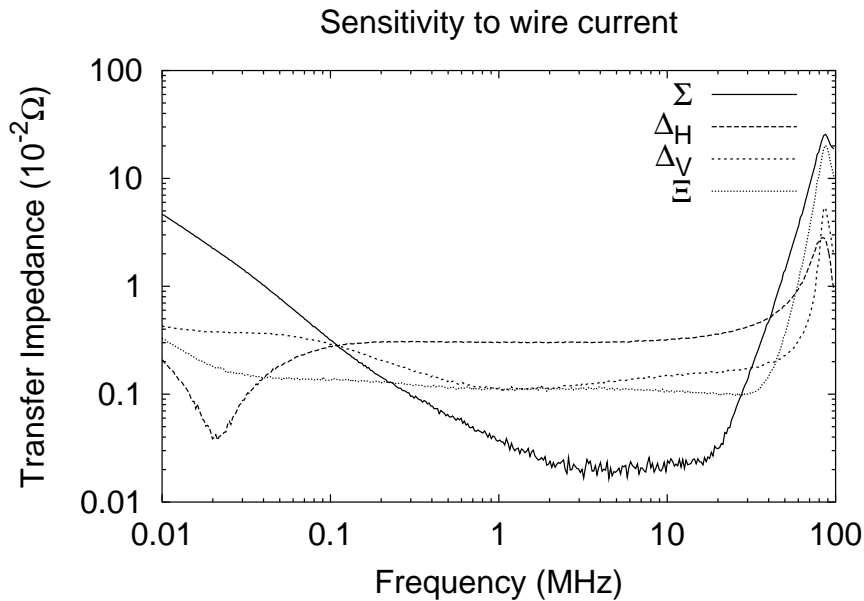

FIGURE 4. Measurement of the common-mode coupling (component independent of position) using a wire movable along the x axis. Ideally, all signals should be zero. The common-mode rejection of the Σ signal is very good up to about 20 MHz, where the tail of the loop resonance begins. The other signal levels are affected by a small (less than 0.5 mm) offset between the electrical and geometrical centre (this is within the error of the absolute wire positioning accuracy). The rise of the Σ signal at low frequencies is an effect of the measurement instrument, that also influences the other measurements slightly. Figure reprinted from [10] with permission from Elsevier Science.
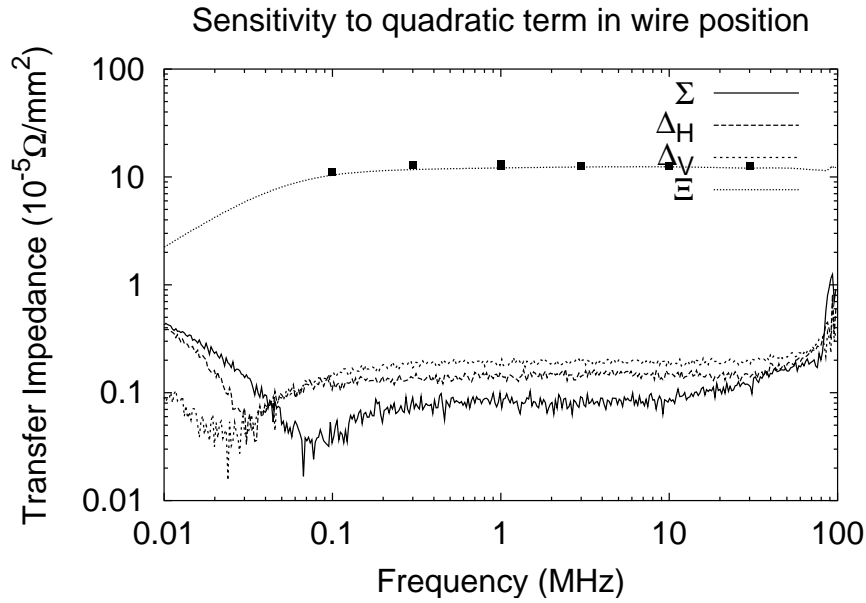
Sensitivity to quadratic term in wire position

FIGURE 5. Measurement of the quadrupole mode coupling using a wire movable along the *x* axis. This is the coupling that is used to measure the quadrupole moment κ. The Ξ response is flat well above 20 MHz (the dots are simulated values for Ξ). Figure reprinted from [10] with permission from Elsevier Science.

The transfer impedances of the pick-up were both simulated and measured in the laboratory (see Figures 4 and 5) with good agreement. As expected, the measured sum transfer impedance is essentially zero in the passband.

Two pick-ups have been installed in consecutive straight sections of the machine. The optical parameters at their locations are given in Table 1. As shown later, it is crucial that the pick-ups are installed at locations with different ratios between horizontal and vertical beta value. The pick-ups were also installed as close as possible to each other to minimize the dependence of their relative betatron phase on the programmed machine tunes and the beam intensity (space charge detuning).

TABLE 1. Optical parameters at pick-up locations. The pick-ups are installed in consecutive straight sections of the PS machine.

Name	β_x	β_y	D_x	$\Delta\mu_x$	$\Delta\mu_y$
QPU 03	22.0 m	12.5 m	3.04 m	0.365	0.368
QPU 04	12.6 m	21.9 m	2.30 m		

SIGNAL ACQUISITION AND TREATMENT

After the hybrids, the composite signals from the two pick-ups are amplified and cabled to Digital Oscilloscopes in an adjacent building. At the maximum sampling rate of 500

Ms/s, 200 turns can be acquired. For normalization purposes, the signal from a wall current monitor is sampled simultaneously, as the pick-ups themselves do not give a measurement of the total beam current. All data treatment is then done on the digitized data. The analysis of the data is made in a LabView program. In order to resolve single bunches, the data is treated in the time domain, considering each bunch passage separately. This is in contrast to earlier measurements in rings, where frequency analysis was always used.

The first step in the analysis is to rid the signal of its intensity dependence, by normalizing to the measured beam current. The analysis is performed in two different ways, depending on whether the position and quadrupole moment are expected to be constant or varying along the bunch.

If there is no variation in position and size along the bunch, and one assumes that the quadrupole pick-up and the wall current monitor have the same frequency response, then the shape of a given pulse must be exactly the same in all signals (apart from a baseline offset and noise effects). The normalization problem then consists in determining the scaling factor between a pulse in the beam current signal and the corresponding pulse on the pick-up outputs.

To do this, time slices of about one RF period centred on the bunch are selected. Each selected slice is a vector of N samples and, under the above assumption, corresponding slices are proportional to each other. The quadrupole moment can therefore be found as the least squares solution to an overdetermined matrix equation, which in the case of the quadrupole signal has the form

$$
\begin{pmatrix} \Sigma_1 & 1 \\ \Sigma_2 & 1 \\ \vdots & \vdots \\ \Sigma_N & 1 \end{pmatrix} \cdot \begin{pmatrix} \kappa \\ c \end{pmatrix} = \frac{Z_\Sigma}{Z_\kappa} \begin{pmatrix} \Xi_1 \\ \Xi_2 \\ \vdots \\ \Xi_N \end{pmatrix} .
\tag{13}
$$

The constant c depends on the base line difference and is not used. The same calculation is performed for the position signals, and the position contribution to the quadrupole moment is then subtracted.

An attractive feature of this method, apart from noise suppression, is that the base line is automatically, and unambiguously, corrected.

However, the assumption that beam size and position is does not vary along the bunch is not always correct. For example, sometimes, only parts of the bunch may oscillate due to a bad injection. Moreover, there is no fundamental reason why the beam size should be constant along the bunch, although this is true for a Gaussian bunch.

If the position varies along the bunch, one can not use the average bunch position to correct the quadrupole moment for its position dependence, since

$$
< x^2 > \neq < x >^2
\tag{14}
$$

The correction must be done point-by-point along the bunch. For this purpose, a second normalization algorithm is used, which first establishes and subtracts the base line, and then calculates the position as well as the quadrupole moment in each point. After this correction, an average beam quadrupole moment can be calculated, but it is also possible to study variations of the beam size along the bunch.

BEAM-BASED CALIBRATION

Apart from calibration measurements in the lab, a number of tests can be performed using the beam, to verify that the pick-ups work as expected.

For example, one can take advantage of the position dependence of the quadrupole moment to make a consistency check between the position and quadrupole moment measurement of the pick-up, using data with large beam position oscillations but stable beam size. Such data can easily be obtained at injection by an appropriate trigger delay, since the beam size oscillations damp away much faster than beam position oscillations. A plot of expected versus measured variation of the quadrupole moment with beam position is shown in Figure 6, showing a good agreement. This test can easily be automated, and is a good indicator of whether the beam position correction works well.
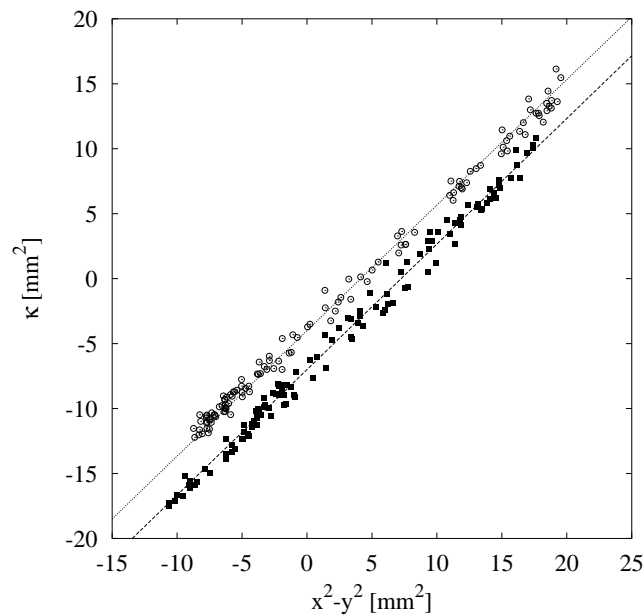

FIGURE 6. Quadrupole moment (uncorrected) versus expected beam position contribution. The squares and circles represent measurements made with the same pick-up on two different beams. The slope of the line is the same in both cases, and is very close to one (0.983). Figure from [11].

Another test is to compare the quadrupole moment measured by the beam with what is expected from the beam emittances measured by other instruments. The standard method for emittance measurement on a circulating beam in the PS is the fast wire-scanner. In order to test the calibration of the pick-ups, measurements were done on several different stable beams, approximately 15 ms after injection. The quadrupole pick-up signal was acquired over 200 machine turns, at the same time as the wire traversed the beam. The comparative measurement was performed on all the operational beams available in the machine, with the exception of the very high intensity beams that saturate the pick-up amplifiers. Thus there was a significant difference in both beam and machine parameters between the different measurements. This was done in an attempt to randomize any systematic errors. The beam parameters are given in Table 2, where the different beams

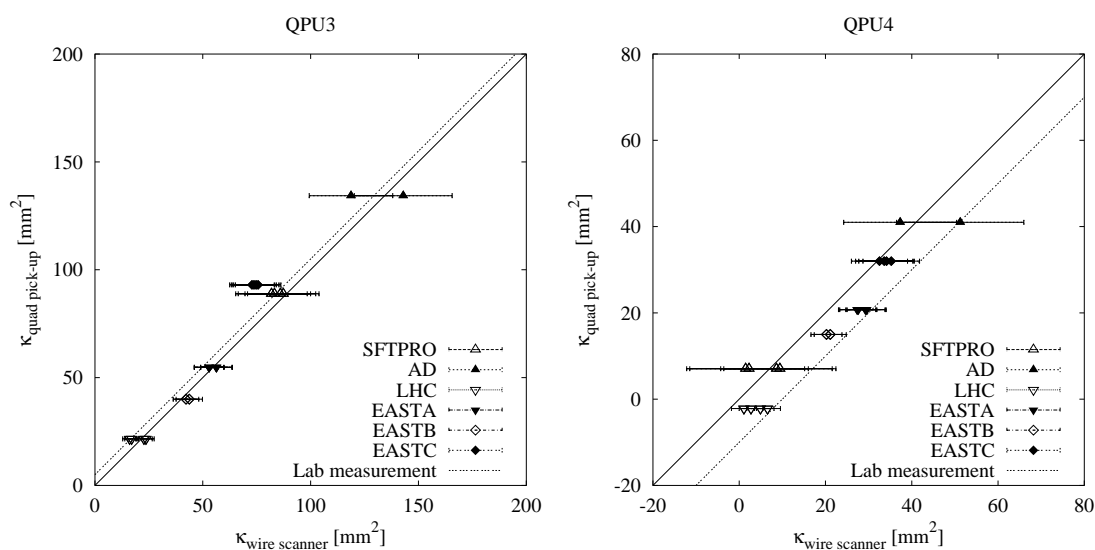| Name	ε_x	ε_y	σ_p	I_{bunch}
SFTPRO	19 μm	12 μm	2.7×10^{-3}	2.7×10^{12}
AD	25 μm	9 μm	2.7×10^{-3}	3.3×10^{12}
LHC	3 μm	2.5 μm	2.2×10^{-3}	6.9×10^{11}
EASTA	8 μm	1.4 μm	2.5×10^{-3}	1.4×10^{11}
EASTB	7.5 μm	1.4 μm	1.6×10^{-3}	8.6×10^{10}
EASTC	12 μm	3 μm	2.4×10^{-3}	4.2×10^{11}

FIGURE 7. Comparison between the measured value from the two quadrupole pick-ups and the expected results calculated from the emittances measured with the wire-scanners. The solid line is the ideal case, and the dotted line includes pick-up offsets measured in the lab prior to installation. All possible ways of combining the wire-scanner measurements are displayed. Note that the cases where the two wire-scanner results are inconsistent are cases with large estimated systematic error. Figure from [11].

have been tagged with their operational names.

The r.m.s. variation in the measured quadrupole moments from turn to turn was of the order of 0.2-0.5 mm^2, depending on the beam intensity. Assuming that the beam size was perfectly stable, this gives an estimate of the single-turn resolution of the pick-up measurement. Also the wire-scanner measurements were stable, although for some beams there was a systematic disagreement between the two wire-scanners measuring in the same plane.

To compare the two instruments, the emittances measured with the wire-scanners were used to calculate the expected quadrupole moment at the locations of the pick-ups. The momentum spread required for both the wire scanner measurement and the subsequent calculation was obtained by a tomographic analysis of the bunch shape[12]. The propagated systematic error in the comparison was estimated on the assumption that the wire-scanner accuracy is 5% in emittance, the beta function at the pick-ups is known

to 5%, the dispersion to 10% and the momentum spread to 3% accuracy. These estimates are rather optimistic, but give considerable propagated errors for certain measurement points. For simplicity, possible correlations between errors (e.g. beta function errors at different locations in the machine) were ignored, and all different error sources were added in quadrature. To accentuate the cases with wire-scanner disagreement, each of the four different ways of combining the two horizontal and two vertical wire-scanners was calculated separately and displayed as separate points. The result is shown in Figure 7.

Overall, the measured data seem to indicate that the offsets are slightly smaller than measured in the lab, which could be explained by the fact that the pick-ups were dismantled in the lab to be moved to the machine. However, the effect is within the error-bar, and no strong conclusion can therefore be made. Moreover, the pick-ups have been dismantled and rebuilt in the lab, without effect on the measured offsets.

The point corresponding to the EASTC beam appears to disagree somewhat in both planes, although the effect is just within the error-bar. There are a number of possible explanations for this that are currently under investigation. The general conclusion from the measurement series is that the wire-scanner and quadrupole pick-up agree within the measurement accuracy. The systematic errors due to optics parameters make it impossible to detect with certainty any difference in pick-up behaviour between the laboratory measurements with a simulated beam, and the measurements on a real beam in the machine. In order to calibrate the pick-ups more accurately using the beam, the wire-scanners and the pick-up should be situated in the same straight section, which is excluded in the PS due to space limitations.

Comparative measurements of injection matching have also been done using a secondary emission (SEM) grid with a fast acquisition system[13], that can measure beam profiles turn-by-turn for a single bunch. This is a destructive device and can only be used in rare dedicated machine development sessions. It is also limited both in bandwidth and
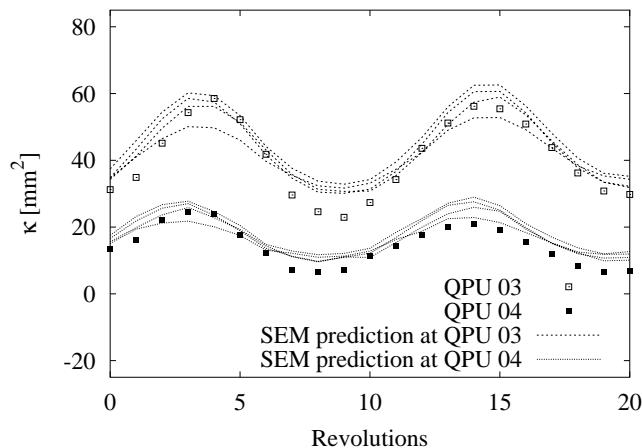

FIGURE 8. Beam size oscillations at injection measured with the quadrupole pick-ups and a turn-by-turn SEM grid. The SEM-grid beam size data were used to calculate the expected quadrupole moment at the pick-up locations. Beam position contributions and known pick-up offsets have been subtracted from the quadrupole moments. Figure from [11].

maximum beam intensity, and therefore it has not been possible to make a full systematic study on beams with different characteristics. Instead, a special beam was prepared, with low intensity to spare the grid, and long bunches due to the bandwidth limitations.

The SEM grid data was used to calculate the expected value of the quadrupole moment at the pick-up locations, using the beta values, dispersion, and relative phase advance in Table 1. The results are shown in Figure 8, and show a rather good agreement with what was actually measured with the pick-ups. The small differences can be accounted for by systematic error sources, i.e. the optical parameters used in the comparison.

EMITTANCE MEASUREMENT

When the circulating beam is stable, the quadrupole moments of a given bunch, as measured by the two pick-ups, are constant and given by

$$
\begin{aligned}
\kappa_1 &= \varepsilon_x \bar{\beta}_{x1} - \varepsilon_y \bar{\beta}_{y1} + \bar{D}_{x1}^2 \sigma_p^2 \\
\kappa_2 &= \varepsilon_x \bar{\beta}_{x2} - \varepsilon_y \bar{\beta}_{y2} + \bar{D}_{x2}^2 \sigma_p^2
\end{aligned}
\tag{15}
$$

When the momentum spread is known, the system of equations can be solved for the emittances, if the ratio between horizontal and vertical beta function is significantly different at the two locations. Thus, measuring the emittance of a stable circulating beam with quadrupole pick-ups is in fact rather straightforward. Such a measurement made in the PS is shown in Figure 9, and compares well with wire-scanner results.

Statistical errors due to random fluctuations in the measurement of κ can, although they are usually small, be reduced by averaging over many consecutive beam passages. The dominant errors are therefore systematic, coming from offsets in the pick-ups and errors in the beta functions, lattice dispersion and momentum spread. The pick-up offsets
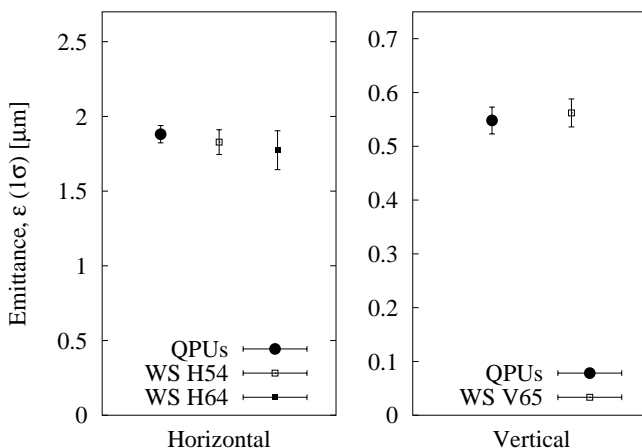

FIGURE 9. Filamented emittance of a proton beam measured with quadrupole pick-ups (QPU) and wire-scanner (WS). There is a good agreement. The error bar is the standard deviation for 10 measurements. Figure reprinted from [14]. ©2001 IEEE.

are, however, known from test bench measurements. Furthermore, by comparing the amplitude and phase of position oscillations as measured by the two pick-ups, the beta ratios and relative betatron phases can be determined.

The main uncertainty is thus the absolute value of the beta function, as for almost any other emittance measurement (e.g. wire-scanner). The accuracy can therefore be expected to be comparable to that of a wire-scanner.

Note that with three pick-ups, suitably located, the momentum spread could also be measured.

MATCHING MEASUREMENT

Even though quadrupole pick-ups can be used to measure filamented emittance, the main reason for installing such instruments in the machine is to be able to measure betatron and dispersion matching at injection, as no other instrument (apart from the destructive SEM-grid) is able to do this. One would like not only to detect mismatch, but also to quantify the injection error in order to be able to correct it.

In a ring, the turn by turn evolution of the beam envelope, and therefore the quadrupole moment, can be expressed in a rather simple analytical formula. If the beam is initially mismatched in terms of Twiss functions or dispersion, the value of κ will vary with the number of revolutions n performed as[15]

$$
\begin{aligned}
\kappa_n = \bar{\beta}_x(\varepsilon_x + \Delta\varepsilon_x) &- \bar{\beta}_y(\varepsilon_y + \Delta\varepsilon_y) + \bar{D}_x^2\sigma_p^2 \\
&+ \bar{\beta}_x\varepsilon_x\delta_{\beta_x}\cos(2\nu_x n - \phi_{\beta_x}) + \bar{\beta}_x\sigma_p^2\delta_{D_x}^2\cos(2\nu_x n - 2\phi_{D_x}) \\
&- \bar{\beta}_y\varepsilon_y\delta_{\beta_y}\cos(2\nu_y n - \phi_{\beta_y}) - \bar{\beta}_y\sigma_p^2\delta_{D_y}^2\cos(2\nu_y n - 2\phi_{D_y}) \\
&\qquad\qquad + \sqrt{\bar{\beta}_x}\sigma_p^2\bar{D}_x\delta_{D_x}\cos(\nu_x n - \phi_{D_x}) \quad (16)
\end{aligned}
$$

assuming linear optics with no coupling between planes. Here, barred parameters refer to properties of the lattice, and $\nu_{x,y} = 2\pi q_{x,y}$.

The two middle lines of Eq. (16) are signal components at twice the horizontal and vertical betatron frequencies. They arise from both dispersion and betatron mismatch. The betatron mismatch is parametrized by the mismatch vector

$$
\vec{\delta}_{\beta_x} = \begin{pmatrix} \frac{\beta_x}{\bar{\beta}_x} - \frac{\bar{\beta}_x\gamma_x + \bar{\gamma}_x\beta_x - 2\bar{\alpha}_x\alpha_x}{2} \\ \frac{\bar{\alpha}_x\beta_x - \alpha_x\bar{\beta}_x}{\bar{\beta}_x} \end{pmatrix} \approx \begin{pmatrix} \frac{\Delta\beta_x}{\bar{\beta}_x} \\ \bar{\alpha}_x\frac{\Delta\beta_x}{\bar{\beta}_x} - \Delta\alpha_x \end{pmatrix} \quad (17)
$$

where, again, the last approximation is valid for small mismatch. The fourth line of Eq. (16) is a signal at the horizontal betatron frequency, which is due to horizontal dispersion mismatch. This is parametrized by the vector

$$
\vec{\delta}_{D_x} = \begin{pmatrix} \frac{\Delta D_x}{\sqrt{\bar{\beta}_x}} \\ \sqrt{\bar{\beta}_x}\Delta D_x' + \bar{\alpha}_x\frac{\Delta D_x}{\sqrt{\bar{\beta}_x}} \end{pmatrix} \quad (18)
$$

There is no corresponding signal at the vertical betatron frequency due to the absence of vertical lattice dispersion. Therefore, it is not possible to distinguish vertical dispersion mismatch from vertical betatron mismatch by studying the quadrupole signal. However, one does not usually expect a large vertical dispersion mismatch.

The first line contains constant terms, and also gives the steady state value that will be reached when the oscillating components have damped away. The steady state (filamented) emittance is given by

$$\varepsilon_x + \Delta\varepsilon_x = \varepsilon_x \frac{1}{2}\left(\bar{\beta}_x\gamma_x + \bar{\gamma}_x\beta_x - 2\bar{\alpha}_x\alpha_x\right) + \sigma_p^2\frac{(\Delta D_x)^2 + (\bar{\beta}_x\Delta D'_x + \bar{\alpha}_x\Delta D_x)^2}{\bar{\beta}_x} \approx$$

$$\approx \varepsilon_x + \varepsilon_x\frac{|\vec{\delta}_{\beta_x}|^2}{2} + \sigma_p^2\frac{|\vec{\delta}_{D_x}|^2}{2} \quad (19)$$

where the last approximation is valid for small betatron mismatch. The emittance increase from mis-steering is not included here, since beam position oscillations filament much slower than beam width oscillations and therefore do not affect the emittance over the first few turns.

By fitting the above function to the data, the injected emittances, the betatron mismatches in both planes, and the horizontal dispersion mismatch are directly obtained. The tunes can also be free parameters in the fit, which automatically estimates and corrects for space charge detuning. An example of a fit to measured data is shown in Figure 10. A requirement for a good fit convergence is, as when measuring filamented emittance, that the ratio between beta functions should be different at the pick-up locations. Also, the tunes must be such that enough independent data points are obtained. In the PS, this means that the working point $Q_h = Q_v = 6.25$, which is close to the bare
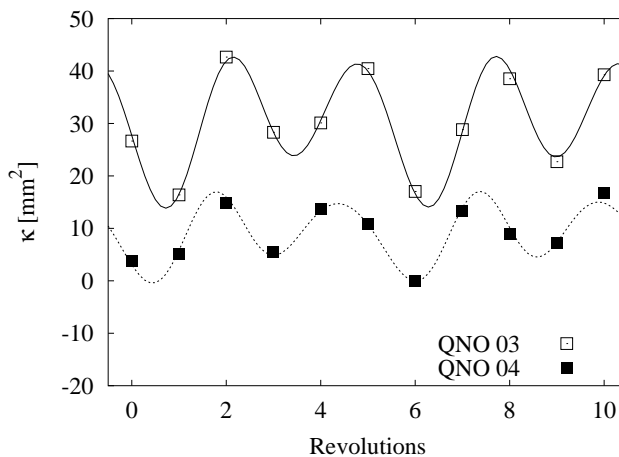

FIGURE 10. Theoretical expression for the quadrupole moment fitted to measured data. Here, seven turns (14 data points) were used to determine 10 free parameters (emittances, betatron and dispersion mismatches, and the tunes), but there is a relatively good match also for the subsequent turns. The measured detuning of the beam width oscillation frequencies were quite significant, $\Delta Q_h = 0.01$ and $\Delta Q_v = 0.05$ (as compared to the tunes measured from position oscillations). Figure from [11].
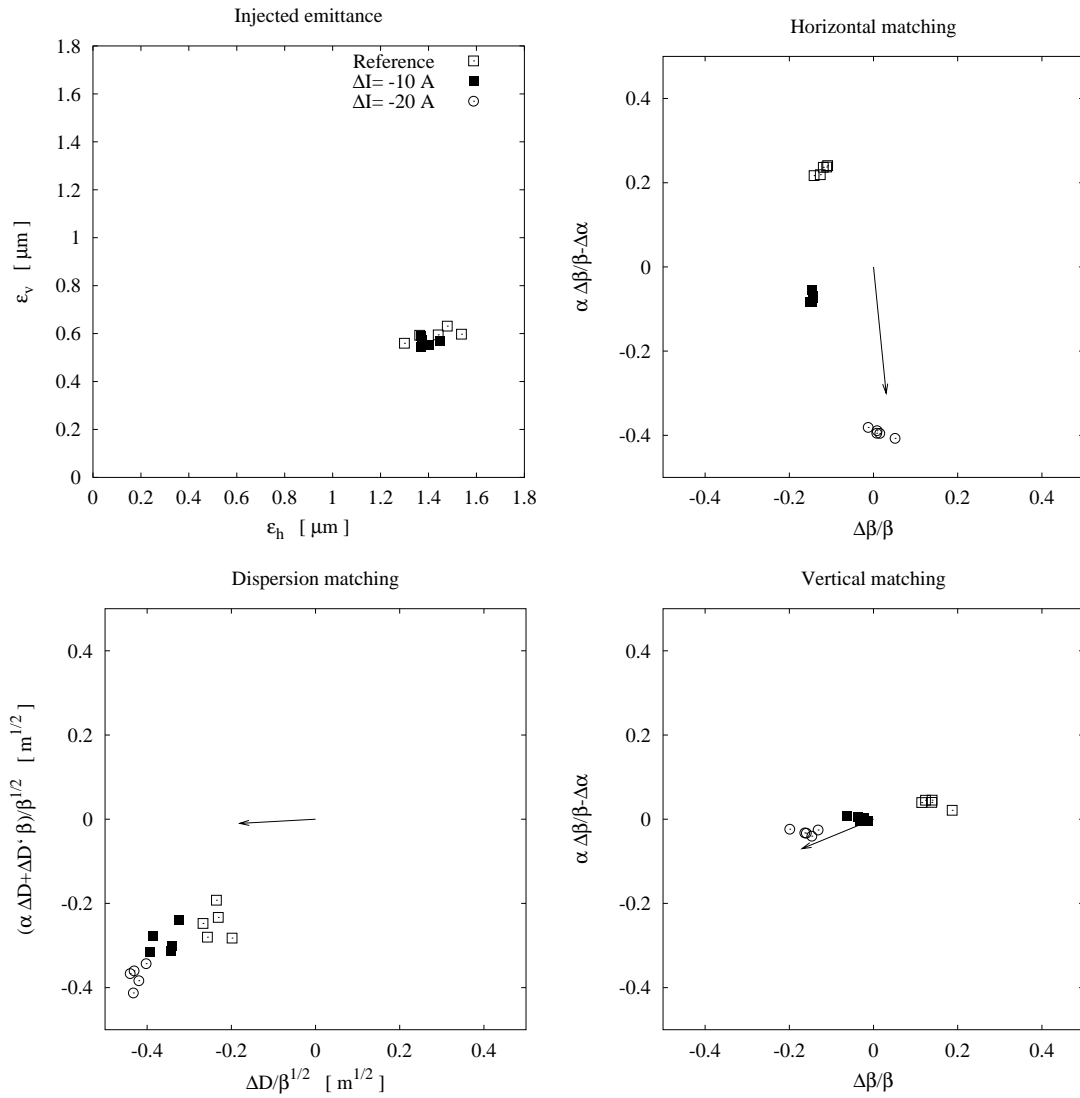
FIGURE 11.   Injected emittance, betatron and dispersion mismatch vectors for three different settings of a transfer line quadrupole. Note the large dispersion mismatch. The vectors illustrate the variation in mismatch that is expected for a correction of -10A (calculated from beam optics theory). There is a good agreement between expected and measured behavior, indicating that the measurement works well. Figure from [11].

tune, should be avoided. With two pick-ups, at least five machine turns (10 data points) are required for the fit, if the tunes are also free parameters. Some more turns can be used to check the error, but the maximum number of turns is limited by decoherence.

Note that since the beam size oscillations due to dispersion mismatch are also detuned by space charge, measuring the dispersion component separately (by changing the energy of the beam and measuring the coherent response) would result in an accumulated phase error in the dispersion term.

To test the injection matching measurement, a series of measurements was done with

different settings of some focusing elements of the PS injection line. An example of such a measurement is shown in Figure 11, where a quadrupole was changed in steps of 10 A, and the resulting variation of the fit parameters recorded. The variation of the different error vectors expected from beam optics theory is also shown, and there is a rather good agreement, both in direction and magnitude of the changes. The injected emittances are unchanged, as expected.

By using the theoretical response matrix for dispersion and betatron matching, a proper correction to the measured error can be calculated[16]. So far, actual corrections of the measured mismatches have not been made, since the dominant error (the dispersion mismatch) can not be corrected without a complete change of optics of the entire line. Studies for a new dispersion-matched optics are underway.

CONCLUSIONS

A new type of quadrupole pick-up has been developed for the CERN PS, and two such instruments are now installed in the machine. The design uses induction loops, coupling to the radial magnetic field component, to separate the small quadrupole signal from the strong common-mode (intensity) signal.

Comparison with other instruments in the machine show good agreement. All observed deviations are within the estimated systematic error bars. The systematic errors come mainly from the imperfect knowledge of beta value and dispersion needed to evaluate the data. Systematic errors are indeed expected to dominate the total error in the quadrupole pick-up measurement, as is the case for most emittance measurement devices.

For matching applications, the pick-ups can be used to determine phase and amplitude of horizontal and vertical betatron mismatch, as well as horizontal dispersion mismatch. This analysis can be done individually on each injected bunch. Since the mismatch is detected as an oscillation, the effect of systematic errors (e.g. pick-up offsets) is not very important.

As emittance measurement devices, the pick-ups have some interesting properties. The single turn resolution makes it possible to measure and follow the evolution of the emittance over many turns (limited only by acquisition memory). When measuring filamented emittance, it possible to reduce the effect of noise by averaging over many turns.

The pick-ups are non-destructive and have no moving parts that wear out, as is the case for a wire-scanner. The can therefore be used on every machine cycle. This makes it possible to create a watchdog application to monitor the evolution of the emittances over a long period, and detect any injection mismatch.

ACKNOWLEDGMENTS

retirement, Lars Søby took over his role and made important contributions, including designing the pick-up amplifiers.

Jean-Mary Roux helped with the mechanical design and made the CAD drawings; Erk Jensen helped with HFFS simulations; Jeroen Belleman gave useful comments on the pick-up design; Uli Raich and Christian Dutriat made sure the wire-scanners and the turn-by-turn SEM-grid were functioning; Michael Benedikt, Christian Carli, Mats Lindroos and the operations team helped set up the beams and participated in some of the measurements. Many others colleagues not mentioned here have also contributed to the project in different ways.

Finally, I would like to thank the organizers of the Beam Instrumentation Workshop for selecting this work for the 2002 Faraday Cup Award.

REFERENCES

1. L. L. Gol'din, *Instruments and Experimental Techniques*, pp. 780–784 (1966).
2. G. Nassibian, The measurement of the multipole coefficients of a cylindrical charge distribution (1970), CERN internal note SI/Note EL/70-13.
3. R. H. Miller, et al., "Non-Invasive Emittance Monitor," in *Proc. 12th Int. Conf. on High Energy Accelerators*, Batavia, IL, 1983.
4. S. J. Russell, *Nucl. Instr. and Meth. in Phys. Res. A*, **430**, 498–506 (1999).
5. S. J. Russell, *Review of Scientific Instruments*, **70**, 1362 (1999).
6. G. Carron, et al., "Measurement of Coherent Quadrupole Oscillations at Injection into the Antiproton Accumulator," in *Proc. 15th Int. Conf. on High Energy Accelerators*, Chicago, IL, 1989.
7. V. Chohan, et al., "Measurement of Coherent Quadrupole Oscillations at Injection into the Antiproton Accumulator," in *Proc. 2nd European Particle Accelerator Conf.*, Nice, France, 1990.
8. F. M. Bieniosek, and K. Fullett, "Measurement and Reduction of Quadrupole Injection Oscillations in the Fermilab Antiproton Accumulator," in *Proc. 16th Particle Accelerator Conf.*, Dallas, TX, 1995, vol. 3, pp. 1942–1944.
9. M. Chanel, "Study of Beam Envelope Oscillations by Measuring the beam transfer function with a quadrupolar pick-up and kicker," in *Proc. 5th European Particle Accelerator Conf.*, Sitges, Spain, 1996, pp. 1015–1017.
10. A. Jansson, and D. J. Williams, *Nucl. Inst. and Meth. in Phys. Res. A*, **479**, 233–242 (2002).
11. A. Jansson, A non-invasive single bunch matching and emittance monitor (2002), physics/0202057, accepted for publication in Phys. Rev. ST-AB.
12. S. Hancock, et al., "Tomographic measurements of longitudinal phase space density," in *Proc. Conf. on Computational Physics*, Granada, Spain, 1998, publ. in: Computer Physics Communications, 118 (1999) 61-70.
13. M. Benedikt, et al., "Injection Matching Studies using Turn by Turn Beam Profile Measurement in the CERN PS," in *Proc. 5th European Workshop on Beam Diagnostics and Instrumentation for Particle Accelerators*, Grenoble, France, 2001.
14. A. Jansson, and L. Søby, "A non-invasive single bunch matching and emittance monitor for the CERN PS," in *Proc. 19th IEEE Particle Accelerator Conf.*, Chicago, IL, 2001.
15. A. Jansson, *Non-Invasive Measurement of Emittance and Optical Parameters for High-Brightness Hadron Beams in a Synchrotron*, Ph.D. thesis, Stockholm University (2001).
16. M. Giovannozzi, A. Jansson, and M. Martini, "Simultaneous Matching of Dispersion and Twiss Parameters in a Transfer Line," in *Proc. Workshop on Automatic Beam Steering and Shaping*, Geneva, Switzerland, 1998, CERN Yellow Report 99-07.